Ginsenoside Rg1 exerts anti-arrhythmic effect by inhibiting I$_{CaL}$ through cAMP-PKA and PI3K-AKT signaling pathways in rat ventricular myocytes after myocardial ischemia-reperfusion injury

Teng Wang[1,2,3,*] (iD)**, Hongyi Zhao**[1,2,3,*]**, Yuting Chen**[1,2,3]**, Sheng Guo**[4]**, Chengzhi Zhou**[4]**, Hong Cao**[1,2,3]**, Qiang Zou**[1,2,3] **and Qingxiu Wang**[5]

Abstract

Objective: Ginsenoside Rg1 has demonstrated beneficial effects in myocardial ische-mia-reperfusion (I/R) injury. However, its potential anti-arrhythmic role in ventricular arrhythmias remains unclear.

Methods: In this study, a whole-cell patch clamp technique was employed to evaluate the effects of Rg1 on L-type calcium current (I$_{CaL}$) and ventricular arrhythmia. Western

[1]Department of Cardiology, Renmin Hospital of Wuhan University, Wuhan, PR China
[2]Cardiovascular Research Institute, Wuhan University, Wuhan, PR China
[3]Hubei Key Laboratory of Cardiology, Wuhan, PR China
[4]Department of Cardiology, Hubei Provincial Hospital of Traditional Chinese Medicine, Hubei University of Chinese Medicine, Wuhan, PR China
[5]Medical Vocational and Technical College of Wuhan University, Wuhan, PR China

*These authors have contributed equally to this work.

Corresponding authors:
Teng Wang, Department of Cardiology, Renmin Hospital of Wuhan University, Wuhan, 430060, Hubei, China.
Email: 595065419@qq.com

Qingxiu Wang, Medical Vocational and Technical College of Wuhan University, Wuhan, 430060, Hubei, China.
Email: 654021404@qq.com

blot analysis was conducted to investigate the underlying signaling pathways involved.
Results: Ginsenoside Rg1 inhibited I_{CaL} in ventricular myocytes in a concentration-dependent manner. Additionally, Rg1 alleviated the I/R-induced increase in diastolic intracellular calcium concentration ($[Ca^{2+}]i$) and reduced calcium overload. Importantly, Rg1 decreased the incidence of ventricular tachycardia (VT) and ventricular fibrillation (VF) in I/R injury models. Mechanistically, these cardioprotective effects appear to be mediated via modulation of the cAMP-PKA and PI3K-AKT signaling pathways.
Conclusions: Rg1 may attenuate the deterioration of cardiac function during acute I/R injury, lower the susceptibility to ventricular arrhythmias, and prevent their occurrence following I/R. These findings suggest that Rg1 holds therapeutic potential in the management of I/R-induced ventricular arrhythmias.

Introduction

Reperfusion therapy has long been recognized as a double-edged sword in the treatment of patients with coronary artery disease. While it effectively restores blood flow to the infarcted myocardium, preserving cardiac tissue and improving both systolic and diastolic function, it may also lead to serious complications, including myocardial ischemia–reperfusion (I/R) injury, heart failure, and life-threatening arrhythmias.[1,2] I/R injury is primarily associated with impaired ventricular systolic function and electrophysiological disturbances that promote ventricular arrhythmias. In particular, reduced contractility may exacerbate electrical heterogeneity in the myocardium, resulting in abnormal conduction velocity and timing, altered restitution of action potential duration (APDR), and electrical alternans.[3] These changes create a highly arrhythmogenic substrate, predisposing the heart to I/R-induced ventricular tachycardia (VT) and ventricular fibrillation (VF).

Calcium ions (Ca^{2+}) are central to myocardial excitation–contraction coupling. Their intracellular concentration is tightly regulated by L-type calcium current (I_{CaL}), which controls calcium influx across the cardiomyocyte membrane and determines the plateau phase of the cardiac action potential.[4] Disruption of I_{CaL} function during I/R contributes to intracellular Ca^{2+} overload and calcium oscillations, both of which are key triggers of ventricular arrhythmias.[5] Therefore, therapeutic strategies aimed at stabilizing ion channel activity and limiting Ca^{2+} overload during reperfusion are essential for reducing the risk of arrhythmias.

Ginseng, a traditional medicinal herb used for thousands of years in countries such as China, Korea, and Japan, contains various biologically active compounds, among which ginsenoside Rg1 (Rg1) is one of the most studied.[6] Rg1 exhibits a wide range of pharmacological activities, including anti-cancer, antioxidant, anti-inflammatory, anti-apoptotic,

and neuroprotective effects, as well as promoting cell proliferation and differentiation.[7–9] Recent research has highlighted the cardioprotective potential of Rg1 in conditions such as myocardial I/R injury, cardiac hypertrophy, and cardiomyocyte apoptosis.[10–12] However, its effects on ventricular arrhythmias, particularly those induced by I/R, remain largely unexplored.

In this study, we aimed to investigate the effects of Rg1 on I_{CaL} and to explore its potential anti-arrhythmic mechanisms in ventricular myocytes following I/R injury.

Materials and methods

Ginsenoside-Rg1 and other agents

Ginsenoside-Rg1 (Cat. No. GB09204, purity ≥98%) was purchased from China Institutes for Food and Drug Control. G-Rg1 was dissolved in Tyrode's solution which contained 135 mM NaCl, 5.4 mM KCl, 1.8 mM CaCl$_2$, 1 mM MgCl$_2$, 0.3 mM NaH$_2$PO$_4$, 10 mM HEPES, 10 mM Glucose. Collagenase type I, proteinase E, bovine serum albumin (BSA), HEPES, choline chloride, EGTA, Na$_2$ATP, CsCl, CsOH were obtained from Sigma (St Louis, MO, USA).

Animals and experimental protocols

All animal procedures were conducted in strict accordance with the National Institutes of Health Guide for the Care and Use of Laboratory Animals and were approved by Laboratory Animal Welfare & Ethics Committee of Renmin Hospital of Wuhan University(Wuhan, China), under approval number WDRM20240136, dated May 8, 2024. Sprague-Dawley rats (8 weeks old, male, 200 ± 30 g, $n = 66$) were obtained from the Hubei Province Center for Disease Control and Prevention (Wuhan, Hubei, China). Animals were housed under specific pathogen-free (SPF) conditions with a 12-hour light/dark cycle, controlled ambient temperature (20 ± 2 °C), and relative humidity of 50–60%. Rats had free access to standard laboratory chow and water. They were allowed to acclimate for 1–2 weeks before experimentation. For all surgical procedures, rats were anesthetized via intraperitoneal injection of 3% pentobarbital sodium at a dose of 50 mg/kg. To prevent coagulation, sodium heparin (500 IU/kg) was also administered intraperitoneally. Animal sacrifice was performed by thoracotomy and excision of the heart under deep anesthesia, ensuring rapid death and minimal suffering.The reporting of this study conforms to ARRIVE 2.0 guidelines (Percie du Sert N et al., 2020).

Experimental protocols

A subset of Sprague-Dawley rats was used to determine the optimal concentration of Rg1 for inhibiting I_{CaL} in normal rat ventricular myocytes and to evaluate the concentration dependence of its effect. Rats were randomly assigned to six groups, one control group and five experimental groups receiving different concentrations of Rg1:20,

40, 80, 160, and 320 mg/L. Another subset of rats was used to establish a myocardial ischemia–reperfusion (I/R) model to assess the effect of Rg1-induced postconditioning (Rg1-IPost) on I/R injury and ventricular arrhythmias. These rats were divided into three groups: control group (hearts were continuously perfused with Tyrode's solution without ischemia), I/R group (hearts were perfused with Tyrode's solution for 30 minutes before ischemia, followed by 30 minutes of global ischemia and 30 minutes of reperfusion), and Rg1-IPost group (ischemia + Rg1-IPost) (hearts were treated identically to the I/R group, except that 40 mg/L Rg1 was added to the Tyrode's solution during the reperfusion phase).

Isolation of ventricular myocytes

Sprague-Dawley rats were anesthetized intraperitoneally with 30% pentobarbital sodium (300 mg/kg) and anticoagulated with sodium heparin (500 IU/kg). After 10 minutes, the heart was excised and rinsed with ice-cold normal saline to remove residual blood. An aortic cannula was inserted and connected to a Langendorff isolated heart perfusion system. The heart was first perfused with Ca^{2+}-free Tyrode solution for 10 minutes, followed by Ca^{2+}-free Tyrode solution containing collagenase I (0.33 mmol/L), proteinase E (0.25 mmol/L), and bovine serum albumin (BSA, 0.25 g/L) for 15 minutes. Subseqently, the hearts were flushed again with Ca^{2+}-free Tyrode solution for 5 minutes. The atria, right ventricle, papillary muscle, and Purkinje fibers were removed, and the free wall of the left ventricle was retained. The left ventricle tissue was placed in Tyrode solution containing 0.2 mmol/L Ca^{2+}, minced, and gently agitated. After incubation for 5 minutes, the supernatant was collected to obtain a suspension of single ventricular myocytes. The cells were centrifuged at 500 r/m for 10 minutes at low speed, the supernatant was discarded, and the cell density was adjusted to 5×10^5/ml using Tyrode's solution supplemented with 0.25 mg/ml BSA and 200 U/ml ampicillin. The isolated cells were then used for electrophysiological measurements via the patch-clamp technique.

Patch-clamp

The suspension of isolated rat ventricular myocytes was added to a cell recording chamber on the stage of an inverted microscope (IX70-122, Olympus, Japan), and allowed to settle and adhere to the chamber surface. To record I_{CaL}, the bath solution contained (in mmol/L): 140 choline chloride, 5 CsCl, 5 glucose, 5 HEPS, $0.5 MgCl_2$, and 1.8 $CaCl_2$. The pipette solution contained (in mmol/L): 10 CsCl, 10EGTA, 10 HEPES, 5 $MgCl_2$, and 4 Na_2ATP. After circulating the bath solution for 10 minutes, whole-cell patch-clamp recordings were performed. Rg1 at various concentrations were applied by perfusion for 10 minutes to evaluate its effect on I_{CaL}. The I_{CaL} current was measured in voltage clamp mode using a digital 700AD/DA converter and 6.0.4 pCLAMP software (Axon Instruments, Union City, CA) for data analysis. The I_{CaL} current magnitude was expressed as current density (pA/pF), and the current–voltage (I–V) relationship curve was plotted.

Langendorff heart preparation and hemodynamic measurement

Rats were anesthetized via intraperitoneal injection of 3% pentobarbital (50 mg/kg). Sodium heparin (500 UI/kg) was also administered intraperitoneally for anticoagulation. Following tracheal intubation, mechanical ventilation was provided using a small animal ventilator. After a median sternotomy, the hearts were rapidly excised and immersed in ice-cold oxygenated (100% O_2) normal saline. Residual blood was flushed out, and aortic cannulation was performed for retrograde perfusion using a Langendorff apparatus (Power Lab/4sp, AD Instruments, Australia). Perfusion was carried out with oxygenated Tyrode's solution containing (in mmol/L) 135 NaCl, 5.4 KCl, 1.8 $CaCl_2$, 1 $MgCl_2$, 0.3 NaH_2PO4, 10 HEPES, and 10 glucose, maintained at 37°C using a thermostatically controlled water circulating system. The sinus node was ablated to eliminate spontaneous pacing, and the heart was paced at a frequency of 5 Hz. The left atrium was excised and a balloon catheter was inserted into the left ventricular cavity. The balloon was inflated with 5 ml of water to maintain consistent volume. Hemodynamic signals were recorded and visualized using AD Instruments software. Perfusion pressure was measured via a pressure transducer connected to the aortic cannula.

Electrocardiographic recording procedure

After the hearts were connected to the Langendorff perfusion system, mean arterial pressure (MAP) was recorded using a contact bipolar platinum microelectrode. The electrical signals were amplified using a signal amplifier, filtered with a bandwidth of 0.3 Hz–1 kHz, and digitized via an A/D converter for acquisition on a personal computer. A bipolar platinum stimulation electrode was positioned on the right ventricular epicardium. An S1–S1 pacing protocol was applied, delivering trains of electrical stimuli at a fixed pacing cycle length. Each pulse had a duration of 2 ms, and pacing was initiated with a pacing interval (PI) of 200 ms. For each PI, 50 consecutive stimuli were applied, followed by a 20-second rest period. MAP and action potential duration at 90% repolarization (APD_{90}) were measured from the last 10 stimuli in each train. The PI was then progressively decreased from 180 ms to 5 ms in stepwise increments.

In the S1–S1 dynamic stimulation protocol, as the PI was progressively shortened, electrical alternans of the action potential began to emerge. Pacing was continued until VT or VF was induced. When APD alternans were observed, pacing was interrupted for 1 minute, and the procedure was repeated twice to directly measure the APD_{90} of consecutive action potentials during alternans. Simultaneously, the diastolic interval (DI) between two consecutive action potentials was calculated as DI = PI-APD_{90}. Based on these measurements, restitution curves of action potential duration (APDR) were constructed, plotting APD_{90} against each corresponding PI and DI. The APDR curve was fitted using the single exponential function: APD_{90} $(y) = y_0 + A_1(1 - e^{(-DI/\tau)})$ where y_0 represents the baseline APD_{90}, A_1 reflects the amplitude of the restitution, and τ is the fast time constant of restitution kinetics. To further analyze the steepness of the restitution curve, we applied a sigmoidal fitting equation: $APD_{90} = a + b/\{1 + \exp[-(DI - c)/d]\}$ where d represents the maximal slope of the restitution curve.

Western blotting

Western blotting was performed to evaluate the expression levels of PI3 K, PKA, and cAMP. Cells were lysed in RIPA buffer supplemented with protease and phosphatase inhibitors. Protein concentration was determined using the BCA assay. Equal amounts of protein (20 μg) were resolved on 10% SDS-PAGE gels and transferred onto PVDF membranes. Membranes were blocked with 5% non-fat milk in TBST for 1 hour at room temperature, followed by overnight at 4°C with the following primary antibodies: anti-PI3 K (1:1000, Affinity), anti-P-PI3 K (1:1000, Affinity),   anti-AKT (1:1000, CST), anti-P-AKT (1:1000, CST), anti-PKA (1:1000, Abclonal), anti-P-PKA (1:1000, Abclonal), and anti-cAMP (1:500, Proteintech Group, Inc). After washing, membranes were incubated with HRP-conjugated secondary antibodies (1:5000, Jackson ImmunoResearch) for 1 hour at room temperature. Protein bands were visualized using an ECL system (Thermo Scientific) and imaged with a ChemiDoc XRS + system (Bio-Rad).Densitometric analysis was conducted using ImageJ, with GAPDH (1:10000, Proteintech Group, Inc) was used as the loading control. Experiments were repeated at least three times.

Statistical analysis

Statistical analysis was performed using IBM SPSS Statistics version 20.0. Comparisons between two groups were conducted using the Student's *t*-test. For comparisons among multiple groups, one-way analysis of variance (ANOVA) was used, followed by Tukey's post hoc test for pairwise comparisons. A *P*-value of less than 0.05 was considered statistically significant for all analyses.

Results

Effect of Rg1 on I_{CaL} in rat ventricular myocytes

Application of Rg1 at various concentrations (20, 40, 80, 160, 320 mg/L) under the same holding potential, significantly reduced the I_{CaL} current density in rat ventricular myocytes. The current–voltage (I–V) relationship curve of I_{CaL} showed a concentration-dependent shift (Figure 1(A) to (F), (G)). Based on fitting with the Hill equation, the half-maximal inhibitory concentration (IC$_{50}$) of Rg1 on I_{CaL} was calculated to be 31.99 ± 2.48 mg/L, with a maximum inhibition rate of $88.72 \pm 4.33\%$ (Figure 1(H)). Accordingly, 40 mg/L was selected as the working concentration of Rg1 for subsequent experiments. Furthermore, the inhibitory effect of Rg1 on I_{CaL} was partially reversible following a 10-minute washout. The I_{CaL} current density recovered from -13.87 ± 4.93 pA/pF to -7.19 ± 0.71 pA/pF ($n = 6$ cells), indicating more than 90% restoration.

Effect of Rg1-IPost on I/R injury in isolated rat heart

In the I/R group, the hearts showed reduced contractility, and the recovery of spontaneous beating was significantly delayed and markedly slowed. The post-reperfusion beating
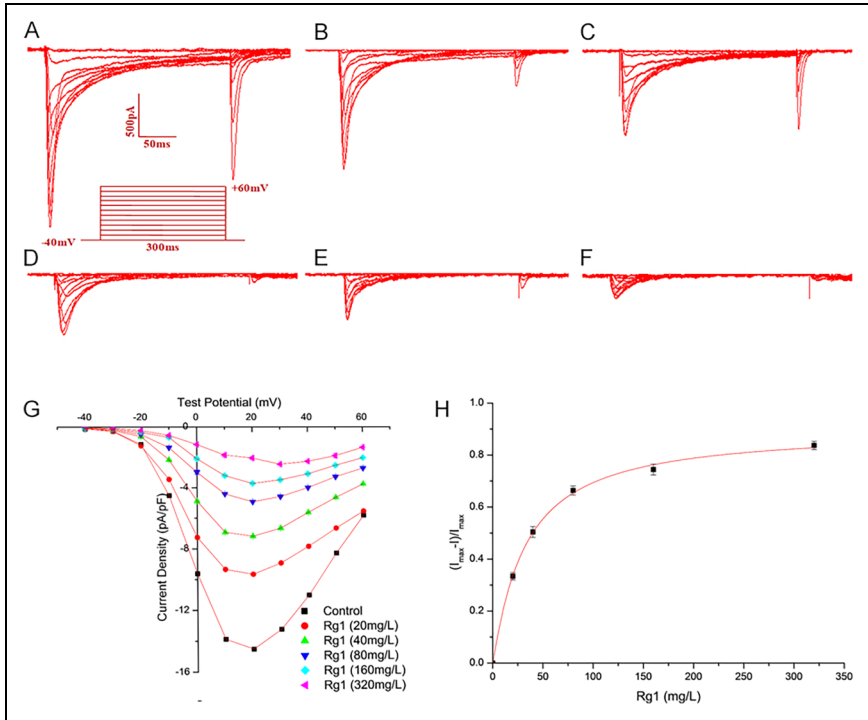
Figure 1. The effects of Rg1 on the L-type calcium current (I_{CaL}) of rat ventricular myocytes, current–voltage relationship, and concentration-dependence in rat ventricular myocytes. (A–F) represent control group (A) and five experimental groups treated with Rg1 at concentrations of Rg1: 20, 40, 80, 160, and 320 mg/L, respectively; (G) shows the effect of Rg1 on the current–voltage relationship curve of I_{CaL}; and (H) shows the concentration-dependence effect of Rg1 on I_{CaL}. (*$P < .05$ vs Control group; #$P < .05$ vs I/R group).

pattern became disordered and irregular (Figure 2(A)). The percentage of left ventricular developed pressure (LVDP) recovery was significantly reduced to $36.28 \pm 3.14\%$, while the magnitude of reperfusion-induced spasm increased to 87.29 ± 7.94 mmHg, indicating that LVDP recovery after I/R was severely impaired (Figure 2(C) and (D)). In contrast, the hearts in the Rg1-IPost group were able to resume beating rapidly, with rhythmic and forceful contractions (Figure 2(B)) The LVDP recovery rate significantly improved to $70.36 \pm 6.42\%$, and the degree of reperfusion spasm was significantly reduced to 13.67 ± 5.67 mmHg, compared with the I/R group ($P < .01$, $n = 10$ hearts) (Figure 2(C) and (D)). These findings suggest that Rg1-IPost exerts a protective effect against myocardial I/R injury.

## Effect of Rg1-IPost on dynamic APDR and slope factor in myocardial I/R injury

In the I/R group, both the pacing interval (PI) and diastolic interval (DI) were significantly reduced, resulting in marked shortening of APD_{90} This accelerated the onset of APDR, as
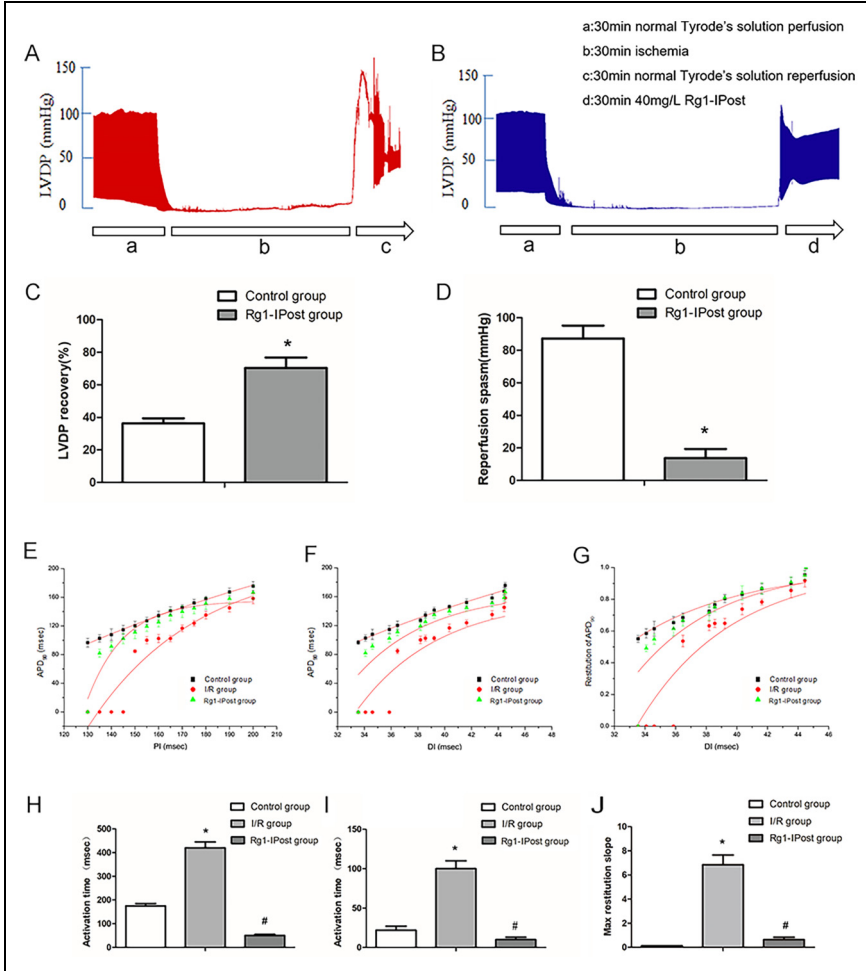
Figure 2. Effects of Rg1-IPost treatments on cardiac function, dynamic action potential duration restitution (APDR), and its slope factor in myocardial I/R injury. (A) and (B) show representative heart function in the I/R group and Rg1-IPost group, respectively. (C) and (D) compare the percentage recovery of left ventricular developed pressure (LVDP) and the extent of reperfusion-induced spasm between the two groups. (E) and (H) show the single exponential function fitting curves of APD_{90} at different pacing intervals (PI) and the corresponding fast time constant (τ). (F) and (I) show the exponential restitution curves of APD_{90} at different diastolic intervals (DI) and the associated τ values. (G) and (J) compare the maximum slope factor (f) of the APD_{90} restitution curve across different diastolic intervals (DI). (*$P < .05$ vs Control group; #$P < .05$ vs I/R group).

indicated by a significantly lower time constant (τ) compared to the control group ($P < .01$, $n = 10$ hearts). The restitution curve exhibited a steep slope, with a slope factor of 6.85, in stark contrast to the shallow slope observed in the control group (slope factor = 0.14, $n = 10$ hearts) (Figure 2(E) to (J)).
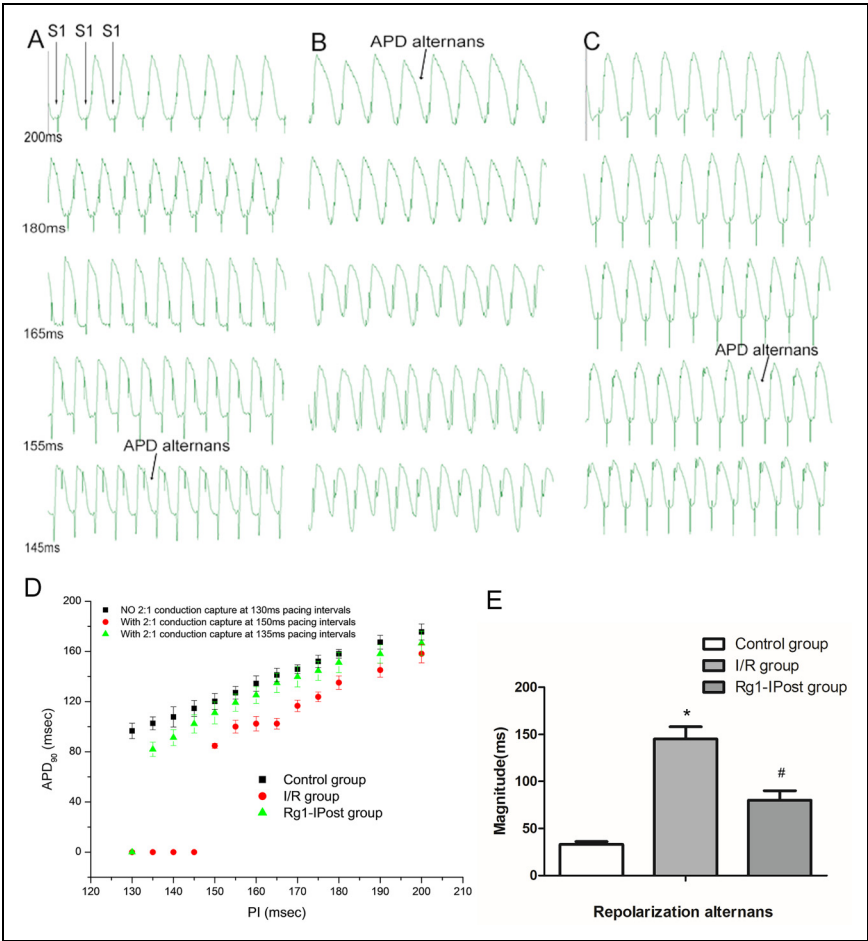
Figure 3. Effects of Rg1-IPost treatment on action potential duration (APD) alternans in myocardial I/R injury. (A, B, and C) show electrical alternans of APD_{90} at different pacing intervals (PI) in the control group, I/R group, and Rg1-IPost group, respectively. (D) illustrates the changes in PI, corresponding APD_{90}, and the occurrence of 2:1 capture in each group. (E) shows the amplitude of APD_{90} alternans, calculated as the difference between the maximum and minimum APD_{90} values in each group. (*$P < .05$ vs Control group; #$P < .05$ vs I/R group).

Effect of Rg1-IPost on the electrical alternans of action potential repolarization and I/R-induced ventricular arrhythmia

In the I/R group, pacing induced a marked increase in the PI at which electrical alternans of action potential repolarization occurred. Alternans began at a PI of 200 ms (Figure 3(A)), and 2:1 capture was observed at a PI of 150 ms—significantly earlier than in the control group, where alternans appeared at a PI of 145 ms and 2:1 capture

was not observed even at PI < 130 ms (Figure 3(A), (B), and (D)). The amplitude of APD$_{90}$ alternans, measured as the difference between the maximum and minimum APD$_{90}$ values, was also significantly greater in the I/R group compared to the control group (143.65 ± 10.30 ms vs 34.01 ± 1.70 ms, $P < .01$, $n = 10$ hearts) (Figure 3(E)).

In the Rg1-IPost group, electrical alternans occurred at a PI of 155 ms, and 2:1 capture was observed at 135 ms—both significantly delayed compared to the I/R group (Figure 3(C) and (D)). The amplitude of APD$_{90}$ alternans in the Rg1-IPost group was significantly lower than that in the I/R group (83.42 ± 8.35 ms, $P < .01$, $n = 10$ hearts), though still higher than in the control group.

In the I/R group, VT or VF was readily induced at a PI of 165 ms, with arrhythmic episodes lasting up to 14.35 seconds. In contrast, the control group exhibited only brief, self-limiting arrhythmias at a PI of 145 ms, lasting approximately 1.4 seconds (Figure 4(A) and (B)). The PI required to induce arrhythmia was significantly prolonged in the I/R group compared to controls (161.37 ± 16.19 ms vs 45.05 ± 9.79 ms, $P < .01$, $n = 10$ hearts) (Figure 4(D)). Moreover, the window of vulnerability (WOV) was significantly widened, and the induction rate of arrhythmia markedly increased (90%, 9/10) compared to the control group (10%, 1/10) ($P < .01$) (Figure 4(E)).

In the Rg1-IPost group, tachyarrhythmia was induced at a PI of 135 ms and lasted 9.4 seconds before spontaneously converting to a regular sinus rhythm (Figure 4(C)). The PI required for arrhythmia induction was significantly shorter than in the I/R group (57.62 ± 13.76 ms, $P < .01$) and not significantly different from the control group ($P > .05$, $n = 10$ hearts) (Figure 4(D)). Additionally, the arrhythmia induction rate was significantly reduced to 30% (3/10) in the Rg1-IPost group (Figure 4(E)).

Effects of Rg1-IPost on I$_{CaL}$ and I–V correlation curve of ventricular myocytes under I/R

Compared with the control group, the I$_{CaL}$ in the I/R group was significantly elevated across all holding voltages (Figure 5(A) and (B)), and the I–V relationship curve of I$_{CaL}$ in ventricular myocytes was markedly shifted downward (Figure 5(D)). At a holding voltage of +20 mV, the current density of I$_{CaL}$ in the I/R group was significantly higher than that in the control group (-11.45 ± 0.32 pA/pF vs -8.92 ± 0.12 pA/pF, $P < .001$, $n = 10$ cells).

In contrast, in the Rg1-IPost group, the I$_{CaL}$ in ischemic ventricular myocytes was significantly reduced at all holding voltages (Figure 5(C)), and the I–V curve shifted upward surpassing even that of the control group (Figure 5(D)). At +20 mV, the current density was reduced to -5.88 ± 0.07 pA/pF ($P < .001$ vs I/R group; $P < .01$ vs control group, $n = 10$ cells).

These results indicate that Rg1-IPost significantly attenuated I$_{CaL}$ in ventricular myocytes following I/R injury, demonstrating a robust inhibitory effect on calcium influx during reperfusion.

Effects of Rg1-IPost on the kinetics of I$_{CaL}$ in ventricular myocytes under I/R

Compared to the control group, the steady-state activation curve of I$_{CaL}$ in ventricular myocytes from the I/R group was significantly shifted to the left (Figure 5(E)), with a
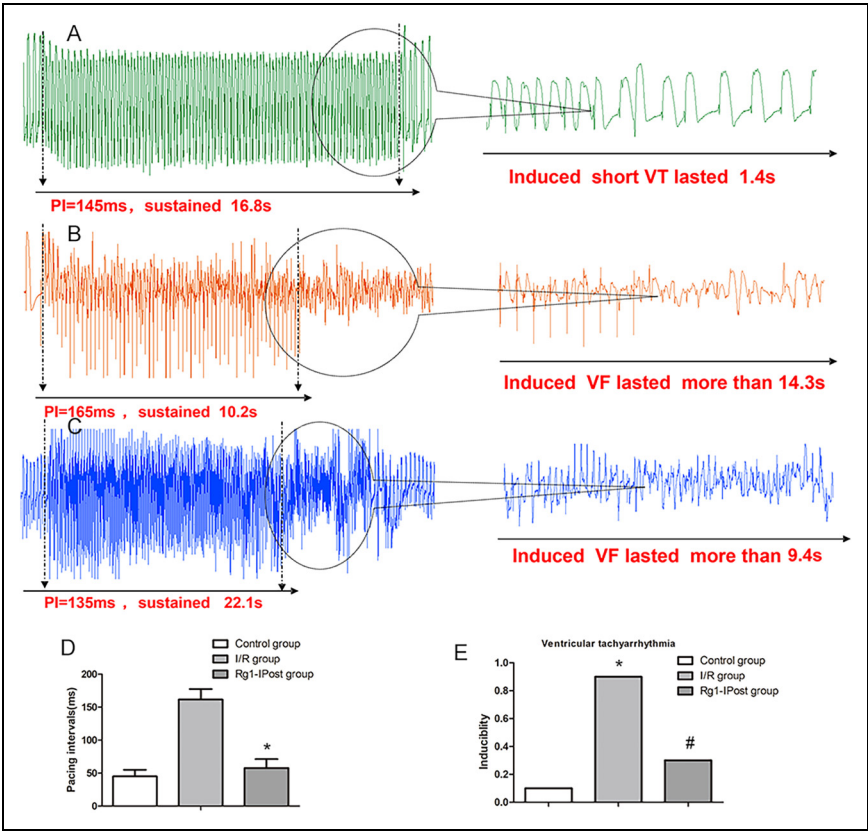
Figure 4. Effects of Rg1-IPost on the induction of ventricular tachycardia (VT) in myocardial I/R injury. (A), (B), and (C) illustrate the types and duration of ventricular tachyarrhythmia induced at different pacing intervals (PI) in the control group, I/R group, and Rg1-IPost group, respectively. (D) shows the comparison of PI thresholds required to induce VT among the three groups. (E) presents the incidence rates of VT in each group.(*P < .05 vs Control group; #P < 0.05 vs I/R group).

notable reduction in both the half-activation potential and the slope factor (P < .001, n = 10 cells; Figure 5(G) and (H)). Meanwhile, the steady-state inactivation curve was shifted to the right, accompanied by increased half-inactivation potential and slope factor; however, these changes were not statistically significant when compared with the control group (P > .05, n = 10 cells).

In contrast, the Rg1-IPost group exhibited a rightward shift in the I_{CaL} activation curve in ischemia-injured ventricular myocytes (Figure 5(E)), with a significantly increased half-activation potential (P < .001 vs I/R group; P > .05 vs control group) and steeper slope factors compared to both the I/R and control groups (P < .001, n = 10 cells). Additionally, the I_{CaL} inactivation curve in the Rg1-IPost group was significantly shifted
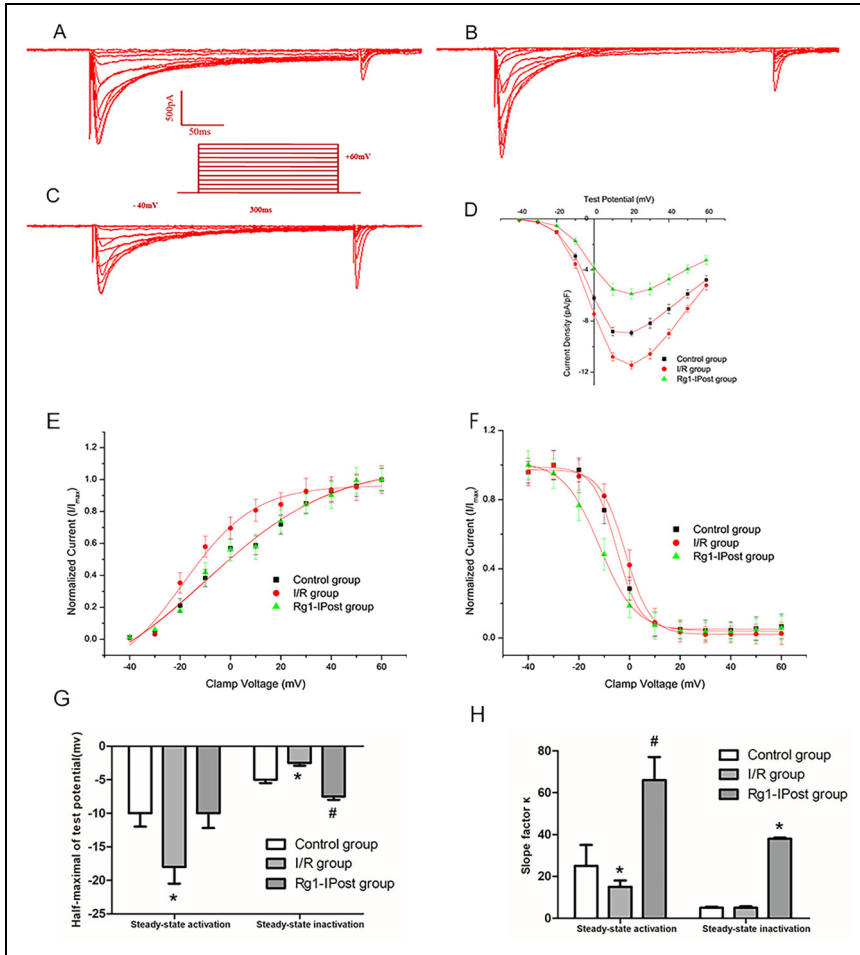
Figure 5. Effects of Rg1-IPost on the I_{CaL}, its I–V relationship curve, and the steady-state activation and inactivation curves of I_{CaL} in ventricular myocytes in myocardial I/R injury. A, B, and C show representative I_{CaL} traces in ventricular myocytes from the control group, I/R group, and Rg1-IPost group, respectively. (D) compares the I–V relationship curve of I_{CaL} in ventricular myocytes among the control group, I/R group, and Rg1-IPost group. (E) and (F) illustrate the steady-state activation and inactivation curves of I_{CaL} in the control group, I/R group, and Rg1-IPost group, respectively. (G) compares the maximum half-inactivation potential of steady-state activation and inactivation in the control group, I/R group, and Rg1-IPost group. (H) presents the slope factor of steady-state activation and inactivation in the control group, I/R group, and Rg1-IPost group. (*P < .05 vs Control group; #P < .05 vs I/R group).

to the left relative to the I/R group (Figure 5(F)). The half-inactivation potential was markedly reduced compared with both the I/R and control groups ($P < .001$, $n = 10$ cells; Figure 5(G)), and the slope factor was significantly increased ($P < .001$, $n = 10$ cells;
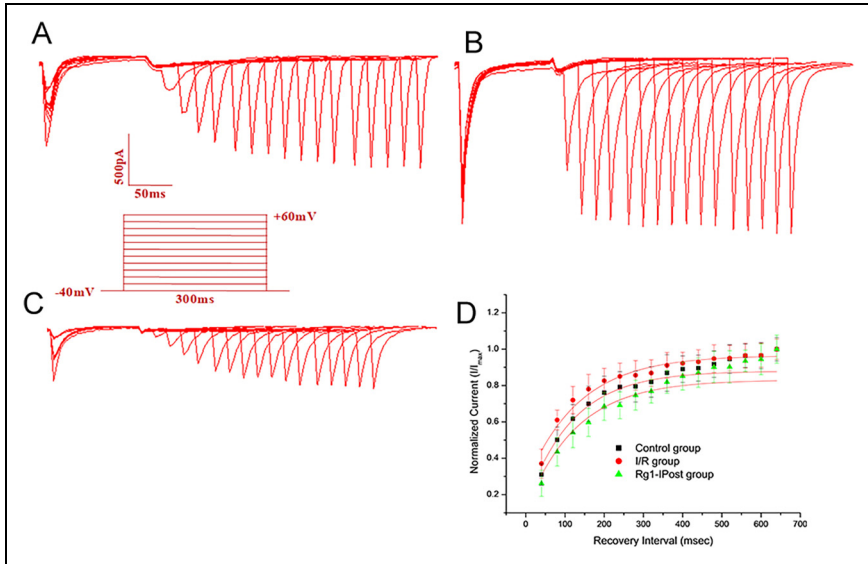
Figure 6. Effects of Rg1-IPost on the steady-state activation and inactivation curves of I_{CaL} in ventricular myocytes following myocardial I/R injury. (A) and (B) shows the steady-state activation and inactivation curves in the control group, I/R group, and Rg1-IPost group, respectively. (C) compares the maximum half-inactivation potential of steady-state activation and inactivation in the control group, I/R group, and Rg1-IPost group. (D) presents the slope factor of steady-state activation and inactivation in the control group, I/R group, and Rg1-IPost group. (*$P < .05$ vs Control group; #$P < .05$ vs I/R group).

Figure 5(H)). These findings indicate that Rg1-IPost significantly modulates both the activation and inactivation kinetics of I_{CaL} in ischemia-injured ventricular myocytes. By promoting channel activation and slowing inactivation, Rg1-IPost may enhance calcium extrusion from the cells into the extracellular space, thereby reducing intracellular Ca^{2+} overload.

Compared with the control group, the recovery current of I_{CaL} from inactivation was significantly elevated in the I/R group (Figure 6(A) and (B)), and the time constant (τ) for rapid recovery from inactivation was significantly shortened (109.51 ± 12.01 ms vs 162.58 ± 17.82 ms, $P < .001$, $n = 10$ cells), resulting in a notably flattened recovery curve (Figure 6(D)).

In the Rg1-IPost group, the I_{CaL} amplitude in ischemic ventricular myocytes was markedly reduced (Figure 6(C)), and the recovery curve became steeper (Figure 6(D)). The time constant for recovery from inactivation was significantly prolonged to 231.16 ± 19.73 ms, which was significantly greater than in both the I/R and control groups ($P < .001$, $n = 10$ cells). These results suggest that Rg1-IPost not only inhibits I_{CaL} amplitude but also delays recovery from inactivation, potentially reducing calcium influx and alleviating calcium overload in ischemic ventricular myocytes.
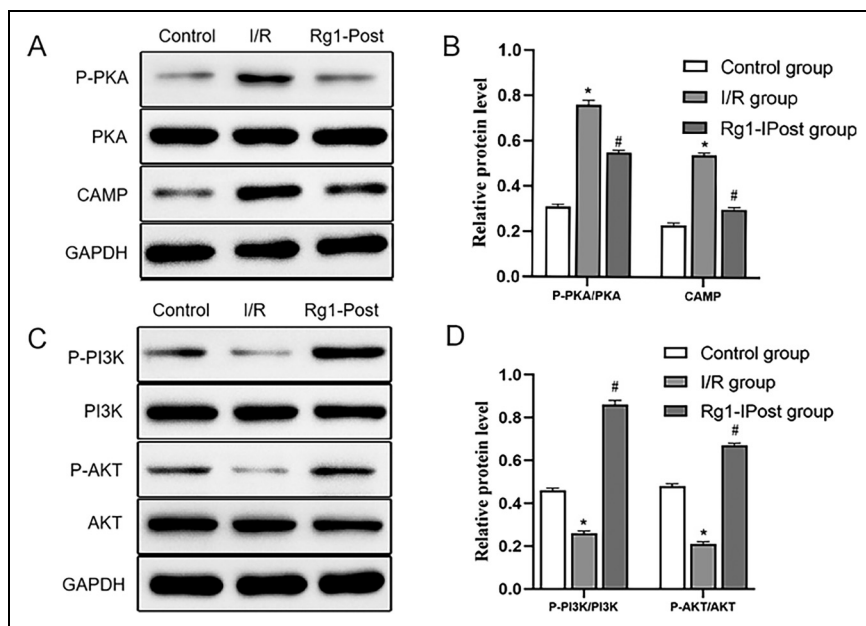
Figure 7. Effects of ginsenoside Rg1 on cAMP-PKA and PI3K-AKT signaling pathways during IR injury. (A) Western blot analysis of cAMP and p-PKA levels in cardiomyocytes following IR injury with or without Rg1 treatment. IR significantly increased cAMP and p-PKA expression, while Rg1 treatment reversed these effects. (B) Quantification of cAMP and p-PKA protein levels normalized to GAPDH as a loading control. (C) Western blot analysis showing the expression of p-AKT and AKT in cardiomyocytes after IR injury with or without Rg1 treatment. IR significantly reduced p-AKT levels, whereas Rg1 treatment increased p-AKT expression, restoring the activation of the PI3K-AKT pathway. (D) Quantification of p-AKT and AKT protein levels normalized to GAPDH ($n = 3$). (*$P < .05$ vs Control group; #$P < .05$ vs I/R group).

Ginsenoside Rg1 acts through cAMP-PKA and PI3K-AKT signaling pathways

To further investigate the potential mechanisms underlying the effects of Rg1, we examined the involvement of signaling pathways known to regulate Ca^{2+} handling, specifically the cAMP/PKA and PI3K-AKT pathways. Our results showed that during I/R injury, the expression levels of cAMP and phosphorylated PKA (p-PKA) were significantly increased; however, treatment with Rg1 reversed these elevations (Figure 7(A) and (B)). Western blot analysis also revealed that I/R significantly decreased the expression of phosphorylated AKT (p-AKT), while Rg1 treatment significantly upregulated p-AKT levels (Figure 7(C) and (D)). These findings suggest that the cardioprotective effects of Rg1 may be mediated through modulation of the cAMP-PKA and PI3K-AKT signaling pathways.

Discussion

In this study, we observed that Ginsenoside Rg1 inhibited I_{CaL} in ventricular myocytes in a concentration-dependent manner, Rg1 shifted the activation curve of I_{CaL} to the right

and the inactivation curve to the left. Additionally, Rg1 demonstrated a cardioprotective effect in the setting of myocardial I/R injury. It effectively reduced I/R-induced elevations in diastolic intracellular calcium concentration ($[Ca^{2+}]i$) and alleviated calcium overload. More importantly, Rg1 significantly decreased the incidence of VT and VF induced by I/R injury.

Reperfusion therapy is a common treatment strategy for patients experiencing acute myocardial infarction. By rapidly restoring blood flow to the ischemic myocardium, it can effectively reduce infarct size, improve clinical outcomes, and lower mortality rates.[13] However, reperfusion itself can introduce new complications, including myocardial reperfusion injury and the development of ventricular arrhythmias.[14]

Myocardial ischemia-reperfusion injury can further impair cardiac function and disrupt the heart's electrical conduction, thereby promoting the development of reentrant ventricular arrhythmias.[15] Moreover, during the reperfusion phase, the concentration of $[Ca^{2+}]i$ during diastole is strongly and positively correlated with left ventricular end-diastolic pressure. Excessive elevations in diastolic $[Ca^{2+}]i$ can lead to hypercontractility of the myocardium, overstretching of cardiomyocytes, and ultimately, cellular injury and degeneration.[16]

Excessive elevation of $[Ca^{2+}]i$ in cardiomyocytes is a key contributor to myocardial I/R injury and ventricular arrhythmias.[17] Consequently, increasing attention has been directed toward the prevention and management of reperfusion-induced ventricular arrhythmias, particularly among emergency and cardiovascular specialists. Pharmacological postconditioning has emerged as an effective strategy for mitigating myocardial I/R injury. Several studies have demonstrated that postconditioning interventions exert cardioprotective effects through multiple mechanisms, including attenuation of calcium overload, reduction of apoptosis, suppression of inflammation, and alleviation of endoplasmic reticulum stress.[18]

Ginsenoside has been used for medicinal purposes in China for thousands of years. Studies have demonstrated their protective effects against IR injury; however, whether ginsenoside Rg1 can attenuate ventricular arrhythmias following acute I/R and the underlying mechanisms remain unclear.[10] In this study, we observed that Rg1 treatment markedly reduced cardiac spasms and shrinkage after 20 minutes of reperfusion. Cardiac systolic and diastolic function recovered more effectively, and left ventricular developed pressure (LVDP) was significantly increased, indicating that Rg1 improves cardiac function in acute I/R and helps protect cardiomyocytes in the peri-infarct region. Furthermore, Rg1 treatment shortened the action potential duration (APD), and increased the action potential amplitude (APA), suggesting more stable electrophysiological properties and improved conduction regularity following Rg1-IPost. Importantly, Rg1 significantly reduced the inducibility of ventricular arrhythmias and shortened the stimulation interval required for arrhythmia induction. These findings indicate that Rg1-IPost effectively reduces the susceptibility to I/R-induced ventricular arrhythmias. This effect may be attributed to Rg1's ability to restore normal systolic and diastolic function, stabilize action potential conduction, and prevent the formation of reentrant circuits, thereby suppressing the onset of reentrant ventricular arrhythmias following acute I/R injury.

Previous studies have demonstrated that post-ischemic increases in cardiac spasticity, delayed recovery of LVDP, prolonged APD, and enhanced susceptibility to ventricular

arrhythmias are closely associated with impaired Ca^{2+} handling in cardiomyocytes. These pathological changes reflect a loss of excitation–contraction coupling integrity and the development of intracellular Ca^{2+} overload.[19,20] A primary contributor to this process is the excessive and rapid activation of I_{CaL} on the cell membrane, which constitute the plateau phase of the action potential and allow substantial influx of extracellular Ca^{2+} into the cytoplasm. In addition, acute ischemia disrupts membrane integrity and alters its permeability further facilitating extracellular Ca^{2+} entry into the cell. This influx may trigger Ca^{2+}-induced Ca^{2+} release, thereby exacerbating cytosolic Ca^{2+} overload. The resulting overload promotes triggered activity, leading to cardiomyocyte injury and arrhythmogenesis.[20] Following myocardial I/R injury, the amplitude of I_{CaL} has been shown to increase significantly, while the I–V curve shifts downward.[19] In contrast, Rg1-IPost treatment significantly reduced I_{CaL} amplitude, with the I–V curve shifting upward and to the right. This reduction in I_{CaL}, along with a slower activation rate, likely contributed to decreased cytosolic Ca^{2+} accumulation, providing a plausible electrophysiological mechanism by which Rg1-IPost mitigates ventricular arrhythmias in the context of acute I/R injury.

The cardioprotective effects of Rg1 may be mediated through multiple signaling pathways, including the cAMP/PKA and PI3 K/AKT pathways. Previous studies have shown that Rg1 can modulate these signaling cascades resulting in improved cardiac function and reduced cardiomyocyte apoptosis.[21–23] The cAMP/PKA signaling pathway plays a pivotal role in regulating myocardial contractility, and calcium handling.[21] Activation of this pathway leads to phosphorylation of L-type calcium channels (LTCCs) enhancing Ca^{2+} influx during the plateau phase of the action potential. While this increase in intracellular Ca^{2+} supports stronger cardiac contractions, excessive activation can promote Ca^{2+} overload, which contributes to arrhythmogenesis. Our findings suggest that Rg1 may suppress I_{CaL}, at least in part, by modulating the cAMP/PKA pathway, thereby limiting Ca^{2+} influx and reducing intracellular Ca^{2+} overload. In addition, the PI3 K/AKT has been reported to regulate various cardiac ion channels, including I_{CaL}.[24] Phosphorylation mediated by PI3 K/AKT signaling may stabilize membrane potential and protect against arrhythmia induction.[25] Our results indicate that Rg1 activates the PI3 K/AKT pathway, contributing to reduced susceptibility to I/R-induced ventricular arrhythmias.The interaction between the cAMP/PKA and PI3 K/AKT pathways—and their regulation by Rg1—may underlie the observed reduction in Ca^{2+} overload and arrhythmia incidence in this study.

Our findings align with previous studies showing that calcium overload and I_{CaL} dysregulation are key contributors to ischemia-reperfusion-induced ventricular arrhythmias.[26] In particular, earlier studies have shown the cardioprotective roles of the cAMP-PKA and PI3K-AKT signaling pathways in modulating calcium homeostasis and membrane electrophysiology.[27,28] Our data confirm and extend these findings by demonstrating that Ginsenoside Rg1 not only inhibits I_{CaL} but also regulates these signaling pathways in the setting of I/R injury. Notably, to the best of our knowledge, this is the first report to systematically evaluate the anti-arrhythmic potential of Rg1 using a combination of electrophysiological, hemodynamic, and molecular approaches in an isolated heart I/R model. This work therefore contributes new mechanistic insight into the

modulation of ventricular arrhythmias and supports the translational potential of Rg1 as a pharmacological postconditioning agent following reperfusion therapy.

Despite the promising findings, our study has several limitations. First, the sample size in each group was relatively small, which may limit the statistical power to detect subtle differences. Larger-scale studies are needed to confirm the observed effects. Second, although we utilized both electrophysiological and molecular approaches in isolated rat hearts, in vivo models and long-term outcome studies were not performed, which may affect the translational relevance. Therefore, while our results suggest a cardioprotective and anti-arrhythmic role of Rg1, the conclusions should be interpreted cautiously, and we propose that Rg1 may represent a promising therapeutic candidate for reperfusion-associated ventricular arrhythmias. Furthermore, we acknowledge that the inhibitory effect of Rg1 on L-type calcium channels was inferred based on electrophysiological data (patch clamp) combined with signaling pathway analysis, rather than through direct binding or structural studies. This indirect approach represents another limitation of our study. Future work involving direct binding assays or channel-specific molecular techniques would help to further validate the mechanism proposed in this study.

Conclusions

Ginsenoside Rg1 may exert cardioprotective effects during ischemia-reperfusion (I/R) injury by reducing L-type calcium current (I_{CaL}), alleviating intracellular calcium overload, and modulating electrophysiological instability. Our findings suggest that Rg1 may attenuate the susceptibility to I/R-induced ventricular arrhythmias, potentially through the regulation of cAMP-PKA and PI3K-AKT signaling pathways. This study provides novel evidence supporting the anti-arrhythmic potential of Rg1 in acute I/R injury. However, further in vivo investigations with larger sample sizes and direct mechanistic studies are required to validate and extend our findings.

Ethical considerations

The present study was approved by the Animal Studies Subcommittee of Wuhan University School of Medicine and was conducted in accordance with the Guide for the Care and Use of Laboratory Animals of the National Institutes of Health.

Declaration of conflicting interests

ORCID iD

Teng Wang 🆔 https://orcid.org/0009-0002-2406-4706

References

1. Ibanez B, James S, Agewall S, et al. 2017 ESC guidelines for the management of acute myocardial infarction in patients presenting with ST-segment elevation. *Eur Heart J* 2018; 39: 119–177.
2. Collet JP, Thiele H, Barbato E, et al. 2020 ESC guidelines for the management of acute coronary syndromes in patients presenting without persistent ST-segment elevation. *Eur Heart J* 2021; 42(141289–1367.
3. Qu Z and Weiss JN. Cardiac alternans: from bedside to bench and back. *Circ Res* 2023; 132: 127–149.
4. Valentim MA, Brahmbhatt AN and Tupling AR. Skeletal and cardiac muscle calcium transport regulation in health and disease. *Biosci Rep* 2022; 42: BSR20211997.
5. Wang R, Wang M, Zhou J, et al. Calenduloside E suppresses calcium overload by promoting the interaction between L-type calcium channels and Bcl2-associated athanogene 3 to alleviate myocardial ischemia/reperfusion injury. *J Adv Res* 2021; 34: 173–186.
6. Shahrajabian MH, Sun W and Cheng Q. A review of ginseng species in different regions as a multipurpose herb in traditional Chinese medicine, modern herbology and pharmacological science. *J Med Plants Res* 2019; 13: 213–226.
7. Gao Y, Li J, Wang J, et al. Ginsenoside Rg1 prevent and treat inflammatory diseases: a review. *Int Immunopharmacol* 2020; 87: 106805.
8. Yang S, Wang J, Cheng P, et al. Ginsenoside Rg1 in neurological diseases: from bench to bedside. *Acta Pharmacol Sin* 2023; 44: 913–930.
9. Qin Q, Lin N, Huang H, et al. Ginsenoside Rg1 ameliorates cardiac oxidative stress and inflammation in streptozotocin-induced diabetic rats. *Diabet Metab Synd Ob* 2019; 12: 1091–1103.
10. Yang C, Jiang G and Xing Y. Protective effect of ginsenosides Rg1 on ischemic injury of cardiomyocytes after acute myocardial infarction. *Cardiovasc Toxicol* 2022; 22: 910–915.
11. Wang X, Wang L, Qi L, et al. Protective effects of ginsenoside Rg1 on acute myocardial infarction. *J Pharm Pharmacol Res* 2020; 4: 44–57.
12. Lu M, Wang J, Sun Y, et al. Ginsenoside Rg1 attenuates mechanical stress-induced cardiac injury via calcium sensing receptor-related pathway. *J Ginseng Res* 2021; 45: 683–694.
13. Zeymer U, Ludman P, Danchin N, et al. Reperfusion therapies and in-hospital outcomes for ST-elevation myocardial infarction in Europe: the ACVC-EAPCI EORP STEMI registry of the European Society of Cardiology. *Eur Heart J* 2021; 42: 4536–4549.

14. Gong FF, Vaitenas I, Malaisrie SC, et al. Mechanical complications of acute myocardial infarction: a review. *JAMA Cardiol* 2021; 6: 341–349.

15. Luqman N, Sung RJ, Wang C, et al. Myocardial ischemia and ventricular fibrillation: pathophysiology and clinical implications. *Int J Cardiol* 2007; 119: 283–290.

16. Gao H, Chen L and Yang H. Activation of α1B-adrenoceptors alleviates ischemia/reperfusion injury by limitation of mitochondrial Ca2+ overload in cardiomyocytes. *Cardiovasc Res* 2007; 75: 584–595.

17. Zhao Y, Sun Y, Zhang L, et al. Prevention of calcium overload-induced myocardial ischemia-reperfusion injury with necrostatin-1 in rats. *Cell Death Discov* 2022; 8: 115.

18. Wu Y, Liu H and Wang X. Cardioprotection of pharmacological postconditioning on myocardial ischemia/reperfusion injury. *Life Sci* 2021; 264: 118628.

19. Sattler SM, Skibsbye L, Linz D, et al. Ventricular arrhythmias in first acute myocardial infarction: epidemiology, mechanisms, and interventions in large animal models. *Front Cardiovasc Med* 2019; 6: 158.

20. Li Q, Huang Y, Xiao Y, et al. ICaI suppression attenuates ischemia-reperfusion-induced ventricular arrhythmias by preventing calcium overload. *Front Cardiovasc Med* 2023; 10: 1094881.

21. Sun X, Gao Y, Li Y, et al. cAMP/PKA signaling modulates calcium handling and prevents ventricular arrhythmias post-myocardial infarction. *Am J Physiol Heart Circ Physiol* 2020; 318: H771–H783.

22. Luo T, Liu H, Tang Q, et al. PI3K/Akt-mediated Cardioprotective effects of ginsenoside Rg1 on ischemia/reperfusion injury: role of mitochondrial dynamics. *J Cell Mol Med* 2023; 27: 1423–1433.

23. Wang H, Li X and Liu C. Ginsenoside Rg1 protects against myocardial ischemia-reperfusion injury by activating the PI3K/Akt pathway and suppressing apoptosis. *Phytomedicine* 2024; 115: 154887.

24. Koh DS, Stratiievska A, Jana S, et al. Genetic code expansion, click chemistry, and light-activated PI3K reveal details of membrane protein trafficking downstream of receptor tyrosine kinases. *Elife* 2024: 12: RP91012.

25. Qin W, Cao L and Massey IY. Role of PI3K/Akt signaling pathway in cardiac fibrosis. *Mol Cell Biochem* 2021; 476: 4045–4059.

26. Tappia PS, Shah AK, Ramjiawan B, et al. Modification of ischemia/reperfusion-induced alterations in subcellular organelles by ischemic preconditioning[. *Int J Mol Sci* 2022; 23: 3425.

27. Ghigo A, Laffargue M, Li M, et al. PI3K And calcium signaling in cardiovascular disease. *Circ Res* 2017; 121: 282–292.

28. Wang Z, Liu D, Varin A, et al. A cardiac mitochondrial cAMP signaling pathway regulates calcium accumulation, permeability transition and cell death. *Cell Death Dis* 2016; 7: e2198–e2198.